

THRESHOLDS FOR EPIDEMIC OUTBREAKS IN FINITE SCALE-FREE NETWORKS

DONG-UK HWANG

Istituto Nazionale di Ottica Applicata
Largo E. Fermi, 6 50125 Florence, Italy

S. BOCCALETTI

Istituto Nazionale di Ottica Applicata
Largo E. Fermi, 6 50125 Florence, Italy

Y. MORENO

Instituto de Biocomputación y Física de Sistemas Complejos (BIFI),
Universidad de Zaragoza, Zaragoza 50009, Spain

R. LÓPEZ-RUIZ

Department of Computer Science,
University of Zaragoza, Zaragoza 50009, Spain

(Communicated by Mingzhou Ding)

ABSTRACT. We numerically investigate the existence of a threshold for epidemic outbreaks in a class of scale-free networks characterized by a parametrical dependence of the scaling exponent, influencing the convergence of fluctuations in the degree distribution. In finite-size networks, finite thresholds for the spreading of an epidemic are always found. However, both the thresholds and the behavior of the epidemic prevalence are quite different with respect to the type of network considered and the system size. We also discuss agreements and differences with some analytical claims previously reported.

1. Introduction. Complex networks have been widely used to describe many relevant situations in social, biological, and communication sciences [1, 2, 3]. These are objects where the nodes represent individuals or organizations, whereas the links model the interaction among them. Relevant examples in which a network approach has contributed to understanding important aspects of the global behavior are the Internet [4], the World Wide Web [5], metabolic networks [6], food webs, protein and neural networks [1], and human sexual contacts [7]. Many complex networks can be used in epidemiology to model the spread of epidemic diseases in population of individuals. A key issue is the characterization of the threshold for epidemic outbreak processes, in view of assessing strategies for vaccination campaigns to be efficient.

Scale-free networks (SFNs) are those complex networks where the probability that a given node has k connections follows a power-law distribution $P(k) \sim k^{-\gamma}$. The thorough characterization of SFNs have allowed investigators to bound the exponent γ between 2 and 3.5 [1]. An immediate consequence is that the fluctuation

2000 *Mathematics Subject Classification.* 92D30.

Key words and phrases. epidemic threshold, scale-free network.

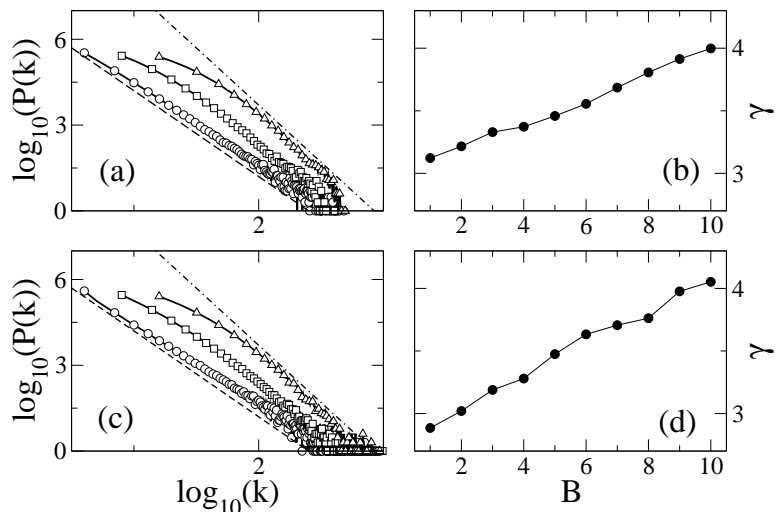


FIGURE 1. Degree distribution $P(k)$ (in logarithmic scale) vs. k (in logarithmic scale) [(a), (c)] and γ coefficient vs. B [(b), (d)]. Here (a) and (b) refer to SFN, and (c) and (d) to SSFN. In (a) and (c), triangles correspond to $B = 10$, squares correspond to $B = 5$, and circles to $B = 0$. The dashed and dot-dashed lines are a schematic drawing of potential scaling laws with $\gamma = 3$ and $\gamma = 4$, respectively.

of connectivities - that is, the second moment of the degree distribution ($\langle k^2 \rangle$) - does not converge in the thermodynamic limit [3], in many cases of practical relevance, for which $\gamma < 3$. Recently, SFNs have been shown to possess very important peculiar properties, such as the absence of a threshold for percolation processes [8], as well as a major propensity for robust synchronization among nodes [9]. Furthermore, SFNs have often been used in the past to model the spread of epidemic diseases in a population of individuals since they properly take into account the actual topology of many real networks where this kind of process occurs [10, 11, 12, 13, 14, 15, 16, 17, 18, 19, 20, 21]. The key model in such epidemiological studies is the susceptible-infected-susceptible (SIS) model [22], where each node represents an individual and each link a connection between two individuals. The nodes here are in a binary state: "healthy" or "infected". At each time step, a healthy node becomes infected at a rate ν only if it is connected with at least one infected node. At the same time, infected nodes are cured at a rate δ (usually and hereinafter $\delta = 1$), thus regaining susceptibility.

The numerical and analytical exploration of the epidemic spreading process, and by extension the percolation one [21, 19], has been a subject of intense research even when degree-degree correlations are introduced [16, 19, 20]. This is usually done by taking a continuous limit and making $N \rightarrow \infty$. However, real networks are always finite and thus they show an effective epidemic threshold [23]. This point has not yet received the due attention in network literature, and extensive numerical simulations on scale-free networks in which epidemic thresholds are reported are not currently available.

The main goal of this paper is to fill that gap. To this end, we use a generalization of the original growing procedure for SFNs, by which the γ parameter can be modulated parametrically and can be made larger than three. Thus, we can control the convergence of connectivity fluctuations in the thermodynamic limit and also report on epidemic threshold values for finite scale-free networks by implementing the SIS model. Furthermore, we study the influence of local network properties, such as the clustering coefficient and the average shortest path length on the critical points characterizing epidemic outbreaks.

2. Epidemic thresholds in SFNs. The absence of an epidemic threshold in scale-free networks was first reported a few years ago in Refs. [10, 11]. The authors showed theoretically by a dynamical mean-field approximation that in SFNs with $2 < \gamma \leq 3$, the unbounded fluctuations of the connectivity distribution imply the lack of an epidemic threshold when $N \rightarrow \infty$. This, in turn, leads to the conclusion that diseases always persist in such networks even when the spreading rate becomes very small [10, 11]. In particular, Refs. [10, 11] have shown that the epidemic threshold is given by $\lambda_c = \langle k \rangle / \langle k^2 \rangle$, thus predicting a vanishing λ_c for all SFNs with $2 < \gamma \leq 3$ as the thermodynamic limit is approached. This result was validated numerically by showing that the survival probability of one infected node in a SFN has a finite value for large enough sizes of the networks under study, even for small spreading rates. Furthermore, the same studies showed that this is not the case for random graph topologies [2], where we have the classic picture of a finite threshold below which no epidemic outbreak occurs. This was taken as a consequence of the convergence of fluctuations in the node's connectivities.

Soon afterward, it was proposed that networks where local properties are strong (in particular, the so-called structured scale-free networks (SSFNs) where the clustering coefficient is of the order of unity) do show a finite epidemic threshold even for a diverging second moment of the degree distribution [15]. In this case, the presence of a finite epidemic threshold was motivated by the high clustering of the SSFN, which prevents such networks from spreading an infection. However, a later study argued that the argument was somehow misled because SSFNs do not possess small-world properties [24], a key property of all known complex networks.

Another interesting contribution to the topic was given in [13]. In this study, the authors introduced a network model exhibiting scale-free properties that could show persistent infections at any spreading rate $\lambda > 0$ for any $\gamma > 1$. Such an alternative flexible model is inspired by the principle of evolutionary selection of common large-scale structure in biological networks. The results were also proved analytically by a more sophisticated mean-field approximation (where previous results are contained) that incorporates connectivity matrices between nodes having k and k' degrees [13].

In summary, one may say that having a scale-free degree distribution with a diverging second moment is a sufficient condition to have a null epidemic threshold in unstructured networks with either assortative or disassortative mixing [12, 16, 19, 20]. The basic assumption of the dynamical mean-field approach is that all vertices within a given degree class can be considered statistically equivalent; therefore, the results do not apply to structured networks in which a distance or time ordering can be introduced (for instance, when the small-world property is lacking).

Finally, we would like to stress that the studies summarized above are aimed at a better comprehension of epidemic processes, since they have at least pointed to new strategies for vaccination campaigns to be efficient. For instance, special

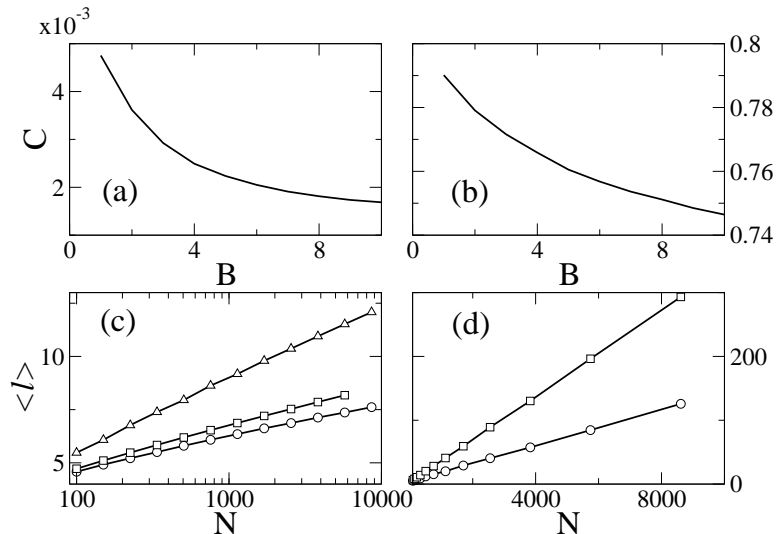


FIGURE 2. Clustering coefficient C vs. B ([a] for SFN, [b] for SSFN) and average path length $\langle \ell \rangle$ vs. the network size N ([c] for SFN, [d] for SSFN). In (c), the horizontal axis is in logarithmic scale; circles correspond to $B = 0$, squares to $B = 10$, and triangles correspond to a SSFN with $B = 10$ and with 10% of randomly selected rewired links. In (d), circles correspond to $B = 0$, and squares to $B = 5$.

policies for curing mostly the highly connected nodes in SFNs were considered in [14]. Such a policy can restore a finite epidemic threshold; thus, it would potentially eradicate a disease. The main result of [14] is that the more biased the policy is toward the hubs, the larger effect it has in bringing the epidemic threshold above the spreading rate.

3. Scale-free networks with initial node attractiveness. In this section, we describe a generalization of the Barabási-Albert(BA) formula that allows more flexibility in the selection of the γ coefficient. Two different types of networks will be used henceforth. The first gives results (i.e., local topological properties) similar to the original preferential attachment procedure [3], but we can tune the exponent beyond $\gamma = 3$. The second model employed has its counterpart in the deactivating procedure leading to the so-called structured scale-free networks [15]. Unless both SFN and SSFN have similar properties in degree distribution, the main local topological features, such as the small-world property and the clustering coefficient, are quite different[24].

3.1. Scale-free networks. We here describe the generalization of the preferential attachment procedure introduced in [3]. We start with m nodes (hereinafter and without lack of generality, we fix $m = 4$) fully connected with each other. Then we add new nodes to the network. At each time step, a new node is added, its degree is fixed to be m . The probability P_i that such new node may be linked with the i -th old node is defined as follows:

$$P_i = \frac{k_i + B}{\sum_j (k_j + B)}, \quad (1)$$

where k_i is the degree of the i -th node, and B is a tunable real parameter, representing the initial attractiveness of each node. This generalization was first proposed by Dorogovtsev and Mendes [25] as a way for generating scale-free networks with tunable degree distributions. Our implementation is somewhat different, since we do not distinguish between incoming and outgoing links. Note that the two procedures are equivalent if we make $A = B + m$ in Dorogovtsev's formula [25]. Besides, for $B = 0$, Equation (1) recovers the original preferential attachment [3], leading to a degree distribution $P(k) \sim k^{-\gamma}$ with $\gamma \approx 3$. Here, we briefly reproduce the derivation of the dependency of γ with B by following the continuum approach introduced in [3]. We assume k_i to be a continuous variable, which changes in time following

$$\frac{\partial k_i}{\partial t} = mP_i. \quad (2)$$

By taking into account that $\sum (k_i(t) + B) = 2mt - m + Bt$, one obtains a solution of (2) as a function of the initial time t_i at which every node is introduced. By further assuming that the t_i values have a constant probability density (nodes are added at equal time intervals, thus $P(t_i) = \frac{1}{m_0+t}$), the probability that a given node has a degree $k_i(t) < k$ is given by

$$\begin{aligned} P[k_i(t) < k] &= P\left(t_i > \frac{(m+B)^{1/\alpha}t}{(k+B)^{1/\alpha}}\right) \\ &= 1 - \frac{(m+B)^{1/\alpha}t}{(k+B)^{1/\alpha}(t+m_0)}, \end{aligned} \quad (3)$$

and the degree distribution can be easily obtained as

$$\begin{aligned} P(k) &= \frac{\partial}{\partial k} P[k_i(t) < k] \\ &= \frac{1}{\alpha} \frac{(m+B)^{1/\alpha}t}{t+m_0} (k+B)^{-(1/\alpha+1)}, \end{aligned} \quad (4)$$

which asymptotically ($t \rightarrow \infty$) gives a power-law degree distribution of the form

$$P(k) \sim A(k+B)^{-\gamma}, \quad (5)$$

with $A = (2 + B/m)(m + B)^{2+B/m}$ and with a tunable exponent $\gamma(B) = 3 + \frac{B}{m}$.

Equation (5) represents the behavior of the degree distribution in the thermodynamic limit. For finite-size networks (having N nodes), it is instead to be expected an exponent γ smaller than the corresponding one at $N = \infty$. Figure 1a shows the change of the slope in degree distribution in log-log domain for various B . Linear fits of the corresponding degree distributions make it possible to calculate the dependence of the γ coefficient. Fig. 1b shows that when B is varied from 0 to 10, γ varies in the range from 3 to 4, for the considered value of N .

Another important parameter characterizing the network topology is the clustering coefficient C . As depicted in Figure 2a, C is also slightly modulated by B ,

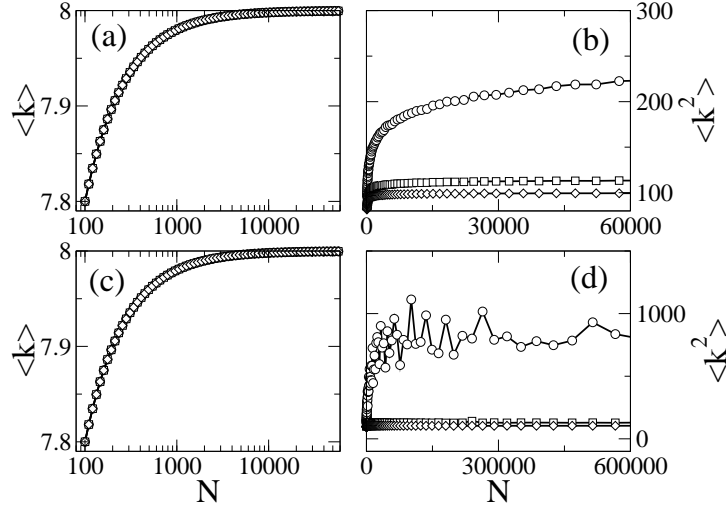


FIGURE 3. First ([a] and [c]) and second ([b] and [d]) moment of the degree distribution vs. N , for SFN ([a] and [b]) and SSFN ([c] and [d]). In (a) and (c), the horizontal axis is in logarithmic scale. In all cases, circles refer to $B = 0$, squares to $B = 5$, and diamonds to $B = 10$.

although remaining very small in all cases. Finally, the small-world property [2] (the fact that the average path length $\langle l \rangle$ scales logarithmically with N) holds for all B values as shown in Figure 2c. The conclusions are that only the degree distribution depends crucially upon the B parameter, whereas other local topological properties, such as the small-world property and the clustering coefficient, are not significantly modified; hence, the topological structure of the network remains unchanged.

An important consequence is the convergence of the second moment of the degree distribution (even taking the thermodynamic limit), which can be made possible by suitably selecting B . In Fig. 3 we report (a) the first moment $\langle k \rangle$, and (b) the second moment $\langle k^2 \rangle$ of the degree distribution as a function of the network size N . While the first moment always approaches $2m$ rapidly, the second moment converges to a finite value only for large B , while for $B = 0$ (the usual SFN case [3]), $\langle k^2 \rangle$ increases indefinitely with N as $\gamma \sim 3$.

3.2. Structured scale-free Network. SSFNs are highly clustered; however, they do not display small-world properties [15] unless rewiring of links is introduced. In these networks, each node can be in two states: "active" or "nonactive". The growing procedure is as follows: The added node is always linked to all m "active" old nodes and is initially set as a new active node. Before adding another new node, one among the $m + 1$ active nodes in the network is deactivated, and the procedure restarts. The probability for deactivating the i -th node is

$$P_i^{de} = \left(\sum_{j \in \mathcal{A}} \frac{1}{k_j + B} \right)^{-1} \frac{1}{k_i + B}, \quad i \in \mathcal{A}, \quad (6)$$

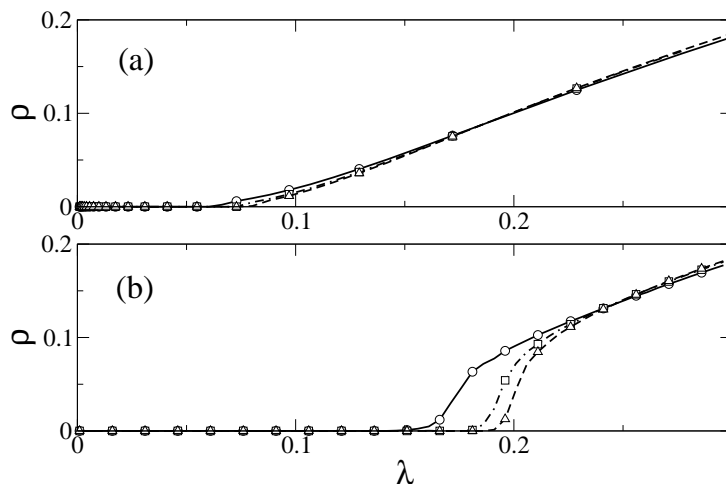


FIGURE 4. Prevalence ρ vs. infection rate λ for (a) SFN and (b) SSFN. Circles refer to $B = 0$, squares to $B = 5$, and upper triangles to $B = 10$. The network size is $N = 30,000$.

where \mathcal{A} is the set of the active nodes. Starting from an initial network of m fully connected active nodes, the above procedure generates a network with an average degree $\langle k \rangle = 2m$ links. Note, however, that there are two different ways in which the addition/deactivation process can be done, leading to two different ranges for the γ values [24, 18]. On the other hand, the exponent γ can be tuned by varying the value of m as well. Here, we keep m fixed to generate networks with the same average connectivity and varied γ by tuning B .

In the case $B = 0$, the degree distribution becomes $P(k) = 2m^2 k^{-\gamma}$, where $\gamma = 3$, and the clustering coefficient $C = 5/6$ [15]. Therefore, the second moment of the degree distribution diverges here in the case $B = 0$. As we increase B from 1 to 10, we numerically found that γ is increasing in the very same way as for SFN; that is, the slope of the degree distribution in the log-log domain changes continuously from 3 to 4 as shown in Figures 1c and 1d.

The clustering coefficient does not show a very significant change with B , as seen in Figure 2b. Finally, B does not affect the scaling properties of the average path length $\langle \ell \rangle$, as depicted in Figure 2d. The average path length grows linearly when we increase the size of the network reflecting the lack of the small-world property for all B values. The numerically measured first and second moments show behavior similar to the case of SFN, and are reported in Fig. 3(d). $\langle k^2 \rangle$ is convergent when B is large enough, and $\langle k \rangle$ converges rapidly to $2m$ for all B values.

In conclusion, we highlight that for both SFN and SSFN, the effect of the parameter B is to tune the scaling exponent of the degree distribution without substantially affecting the other relevant topological parameters. This means that we can use the above approach to test the existence of a threshold in the SIS model for both the case of convergent and divergent fluctuations.

4. Prevalence and threshold for epidemic outbreak. In this section, we implement the SIS model in both SFN and SSFN grown with the procedure described above. In the SIS model, each node of the network is in a binary state: "healthy"

or "infected". At each time step, a healthy node becomes infected with probability λ only if it is connected with at least one infected node, while infected nodes are cured regaining susceptibility for the next step. The prevalence ρ is defined as the average ratio of infected nodes to total nodes in the steady state. Naturally, the prevalence ρ is a function of the infection probability λ . The epidemic threshold λ_c is the point in the phase diagram below which diseases cannot produce a major epidemic outbreak or an endemic state. Notice that the model differs from the susceptible-infected-removed (SIR) model, but the results are equivalent [17, 20, 21].

4.1. Numerical results. Initially, we fixed the network size at $N = 30,000$ and measured the prevalence in various cases for both SFN and SSFN, by varying the B parameter. For each calculation of ρ , twenty different realizations of the same network were used for ensemble averaging, while initial conditions were always put such that 10% of randomly selected nodes are infected at $t = 0$. The dynamics is then evolved for a transient time until $t = 3,000$. At this point, averages for the infection ratio are calculated, taking its value in the next one hundred time steps.

The critical point λ_c for an epidemic outbreak as a function of the network size was obtained by computing the prevalence with twenty different realizations of the same network and five different initial conditions for a given spreading rate λ . For each B value, the network size is increased from 5,000 to 100,000. We furthermore define an effective threshold $\rho^{eff} = n_c/N$, where $n_c = 100$ and N is the total number of nodes. The thresholds λ_c are then calculated as the values at which ρ is sufficiently close to the effective threshold ($|\rho^{eff} - \rho| < \varepsilon$) by bi-section method. However, in most cases, ρ does not reach ρ^{eff} because of limited resolution attributable to the size of the network. In these cases, the threshold λ_c is chosen to be the value for which the minimum prevalence for a given network size is attained.

A few comments are necessary when computing the epidemic threshold λ_c . The first concerns the resolution of ρ , which improves as the network size N increases (of the order of $1/N$); thus, the probability of hopping from a state having finite infected nodes to a state of fully healthy nodes decreases. The second regards the initial density of infected nodes. While for SFNs there is no evidence that the prevalence, and thus the critical point, depends on $\rho(t = 0)$, studies of the SIS dynamics showed that this is not the case when SSFNs are considered [18]. In any case, this dependency is rooted in the way SSFNs are generated [24, 18], a problem that does not arise here as we are generating the networks by tuning B .

Because of the finite-size effect, a finite threshold for an epidemic outbreak appears as shown in Figure 4, where we show the prevalence as a function of the spreading rate λ . The case of SFN is reported in Figure 4 a, where one can see that the slope of ρ continuously vanishes in the vicinity of the threshold, as λ approaches zero. These thresholds are slightly different for various B . In [11], analytical arguments correctly anticipated that when $3 < \gamma < 4$, there are no critical fluctuations around the thresholds, because of the vanishing slope of the order parameter ρ near the critical point. Our results provide the first numerical test to their calculations. At variance, the case of SSFNs (reported in Figure 4) shows a prevalence that suddenly decreases near the threshold.

Our results show that SFNs display continuously decreasing values of λ_c for all B values, even though the decreasing rates are different, as shown in Figure 5. For the same N , the case $B = 0$ (the original SFN) has the smallest threshold values, while the case $B = 10$ shows the largest ones. Notice that, at least up to the maximum

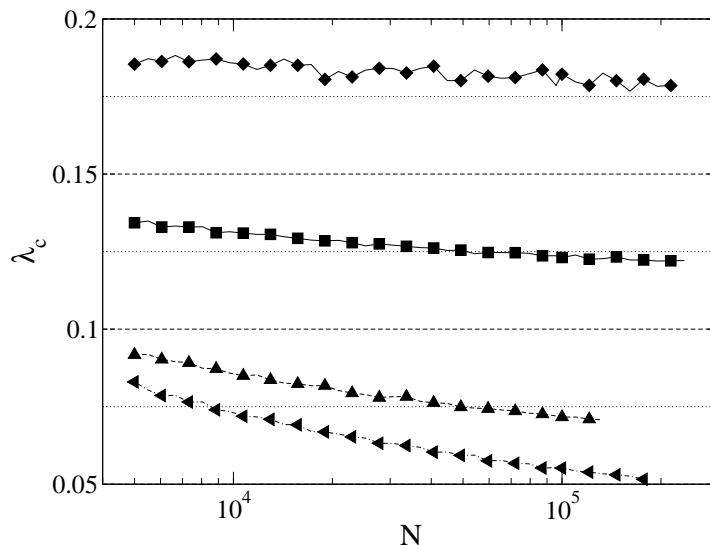


FIGURE 5. Threshold λ_c for epidemic outbreak in the network vs. network size N . Diamonds refer to SSFN with $B = 10$, upper triangles to SFN with $B = 10$, and left triangles to SFN with $B = 0$. Squares correspond to SSFN with $B = 10$ and with 10% of randomly selected rewired links.

size allowed by our numerical capability, there is no qualitative difference between the SFN cases with $B = 0$ (left triangles) and with $B = 10$ (upper triangles), as one should have instead expected from the formula $\lambda_c \propto \langle k \rangle / \langle k^2 \rangle$ derived from a mean-field approach. In comparing the upper triangles curve in Figure 5 with the diamond curve in Figure 3 b, one further notices that such a disagreement holds within a range of network sizes for which the second moment $\langle k^2 \rangle$ of the degree distribution has already numerically converged, thus indicating that the epidemic threshold in finite-size SFNs cannot be solely related to the ratio between the mean degree and the degree fluctuations.

In the case of SSFNs, as N increases, the epidemic threshold decreases much slower than the case of SFNs within the statistical errors. As noted recalled, the original SSFN does not have small-world properties, and this can in part explain the reasons for such a difference in the asymptotic behavior for the epidemic threshold [24]. One can implement the small-world property, by randomly rewiring a given percentage of links. In the case $B = 10$, we operated such rewiring procedure, giving each link a rewiring probability $P_{re} = 0.1$. The rewired network now shows a much faster decreasing threshold for epidemics, similarly to what occurs for SFNs at the same γ value.

The comparison between the results obtained for SFNs and the structured ones for the same γ and system size indicates that the differences in the local properties of both types of networks do affect the way in which the epidemic threshold is approached. The BA network shows a smooth behavior near the epidemic outbreak, while for structured ones the order parameter ρ suddenly decreases when λ_c is approached from the right, signaling two distinct behaviors. Additionally, Figure 5 shows that for finite-size networks, which are the ones we found in the real world,

the structure significantly affects the effective values λ_c for an epidemic outbreak to occur. In particular, we found that structured scale-free networks are always (i.e., independent of the lack or of the small-world property) more resistant to endemic states than the BA-like networks, as they show larger threshold values.

5. Conclusions. We have numerically investigated the existence of a threshold for epidemic outbreaks in two classes of scale-free networks. By tuning the scaling exponent characterizing the degree distribution, we numerically calculated the epidemic thresholds when γ lies in the interval $[3, 4]$. The results confirm the previous analytical arguments about the lack of an epidemic threshold in scale-free networks with diverging fluctuations in the degree distribution. At the same time, we also showed that when $\gamma > 3$, the behavior of an epidemic threshold is a monotonically decreasing function within the same range of network sizes for which the second moment of the degree distribution is numerically convergent.

Finally, we have shown that nonzero thresholds for the spreading of epidemics are always found in finite-size networks; however, the behavior of such thresholds can be strongly influenced by the value of γ and the local properties of the network, making the small-world property more influential than the specific value of the exponent in the degree distribution.

Acknowledgments. This research was partially supported by the post-doctoral fellowship program of the Korea Science and Engineering Foundation(KOSEF), and MIUR-FIRB project no. RBNE01CW3M-001. Yamir Moreno is supported by MCyT through the Ramón y Cajal program.

REFERENCES

- [1] R. Albert and A.-L. Barabási, Statistical mechanics of complex networks. *Rev. Mod. Phys.* 74 (2002) 47-97.
- [2] D.J. Watts and S. H. Strogatz, Collective dynamics of 'small-world' networks. *Nature* 393 (1998) 440-442.
- [3] A.-L. Barabási and R. Albert, Emergence of Scaling in Random Networks. *Science* 286 (1999) 509-512.
- [4] L.A.N. Amaral, A. Scala, M. Barthélémy and H.E. Stanley, Classes of small-world networks. *Proc. Natl. Acad. Sci. U.S.A.* 97 (2000) 11149-52.
- [5] R. Albert, H. Jeong and A.-L. Barabási, Internet: Diameter of the World-Wide Web. *Nature* 401 (1999) 130-131.
- [6] H. Jeong, B. Tombor, R. Albert, Z.N. Oltvar and A.-L. Barabási, The large-scale organization of metabolic networks. *Nature* 407 (2000) 651-654.
- [7] F. Liljeros, C.R. Edling, L.A.N. Amaral, H.E. Stanley and Y. Aberg, The web of human sexual contacts. *Nature* 411 (2001) 907-908.
- [8] R. Cohen, K. Erez, D. ben Avraham and S. Havlin, Resilience of the Internet to Random Breakdowns. *Phys. Rev. Lett.* 85 (2000) 4626-4628 ; D.S. Callaway, M.E.J. Newmann, S.H. Strogatz and D.J. Watts, Network Robustness and Fragility: Percolation on Random Graphs. *Phys. Rev. Lett.* 85 (2000) 5468-5471 .
- [9] M. Barahona, and L. M. Pecora, Synchronization in Small-World Systems. *Phys. Rev. Lett.* 89 (2002) 054101.
- [10] R. Pastor-Satorras and A. Vespignani, Epidemic Spreading in Scale-Free Networks. *Phys. Rev. Lett.* 86 (2001) 3200-3203.
- [11] R. Pastor-Satorras and A. Vespignani, Epidemic dynamics and endemic states in complex networks. *Phys. Rev. E* 63 (2001) 066117.
- [12] M. Boguñá and R. Pastor-Satorras, Epidemic spreading in correlated complex networks. *Phys. Rev. E* 66 (2002) 047104.
- [13] D. Volchenkov, L. Volchenkova and Ph. Blanchard, Epidemic spreading in a variety of scale-free networks. *Phys. Rev. E* 66 (2003) 046137.

- [14] Z. Dezső and A.-L. Barabási, Halting viruses in scale-free networks. *Phys. Rev. E* 65 (2002) 055103.
- [15] V. M. Eguíluz and K. Klemm, Epidemic Threshold in Structured Scale-Free Networks. *Phys. Rev. Lett.* 89 (2002) 108701.
- [16] M. Boguñá, R. Pastor-Satorras and A. Vespignani, Absence of Epidemic Threshold in Scale-Free Networks with Degree Correlations. *Phys. Rev. Lett.* 90 (2003) 028701.
- [17] Y. Moreno, R. Pastor-Satorras, and A. Vespignani, Epidemic outbreaks in complex heterogeneous networks. *Eur. Phys. J. B* 26 (2002) 521-529.
- [18] Y. Moreno, and A. Vázquez, Disease spreading in structured scale-free networks *Eur. Phys. J. B* 31 (2003) 265-271.
- [19] A. Vázquez, and Y. Moreno, Resilience to damage of graphs with degree correlations. *Phys. Rev. E* 67 (2003) 015101.
- [20] Y. Moreno, J. B. Gómez, and A. F. Pacheco, Epidemic incidence in correlated complex networks. *Phys. Rev. E* 68 (2003) 035103.
- [21] M. E. J. Newman, The Structure and Function of Complex Networks. *SIAM Review* 45 (2003) 167-256.
- [22] N.T.J. Bailey, *The mathematical Theory of Infectious Diseases* (Griffin, London, 1975); J.D. Murray, *Mathematical Biology* (Springer Verlag, Berlin, 1993).
- [23] R. Pastor-Satorras and A. Vespignani, Epidemic dynamics in finite-size scale-free networks. *Phys. Rev. E* 65 (2002) 035108.
- [24] A. Vázquez, M. Boguñá, Y. Moreno, R. Pastor-Satorras and A. Vespignani, Topology and correlations in structured scale-free networks. *Phys. Rev. E* 67 (2003) 046111.
- [25] S. N. Dorogovtsev and J. F. F. Mendes, *Evolution of Networks. From Biological Nets to the Internet and the WWW*, Oxford University Press, Oxford, U.K., (2003).

Received on October 21, 2004. Revised on February 24, 2005.

E-mail address: duhwang@ino.it

E-mail address: stefano@ino.it

E-mail address: yamir@unizar.es

E-mail address: rilopez@unizar.es